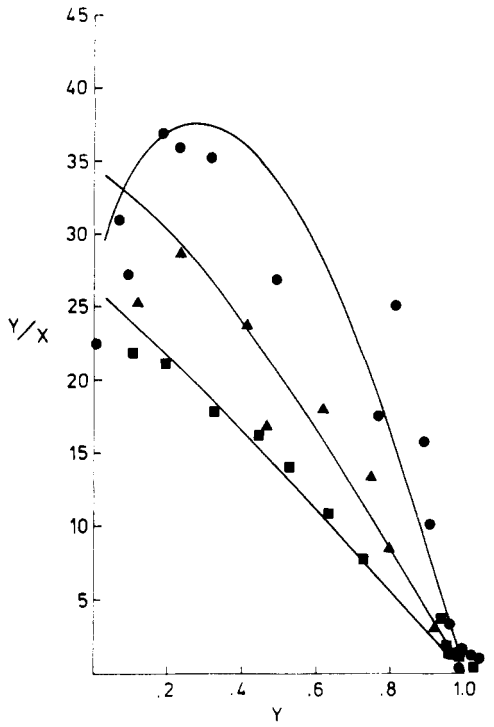

FIGURE 2: Nicotine inhibition of [^{3}H]AcCh binding to solubilized AcChR. Lines are theoretical curves generated from eq 4. Deviation in observed binding and theoretical curves are given as χ_Y^2 and $\chi_{Y/X}^2$. Uninhibited binding (●), $\chi_Y^2 = 0.068$ and $\chi_{Y/X}^2 = 4.202$; 5×10^{-7} M (▲), $\chi_Y^2 = 0.020$ and $\chi_{Y/X}^2 = 1.673$; 1×10^{-6} M (■), $\chi_Y^2 = 0.009$ and $\chi_{Y/X}^2 = 0.217$. Binding constants for AcCh: $K_R = 1.2 \times 10^{-8}$ M, $c = 0.05$, and $L = 2.5$; and for nicotine: $K_{Ri} = 5 \times 10^{-7}$ M, $c_i = 0.1$.

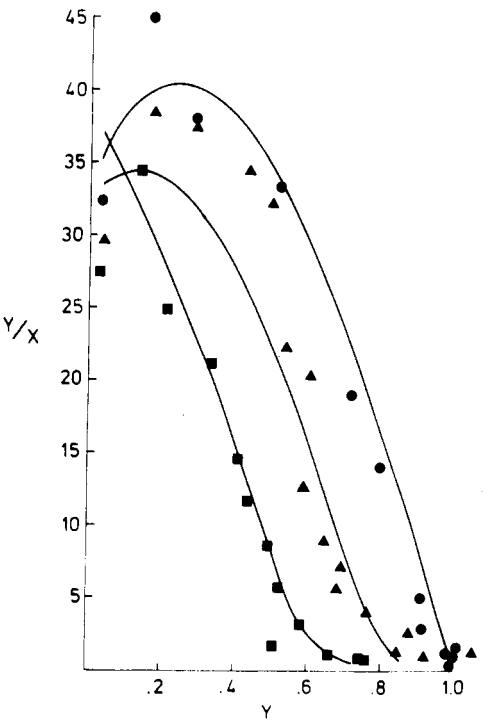

FIGURE 3: Inhibition of [^{3}H]AcCh binding to solubilized AcChR by *d*-tubocurarine. Lines are theoretical curves generated by eq 8 of model III. Deviation in observed binding and theoretical curves are given as χ_Y^2 and $\chi_{Y/X}^2$. Uninhibited binding (●), $\chi_Y^2 = 0.025$ and $\chi_{Y/X}^2 = 1.589$; 10^{-7} M dTC (▲), $\chi_Y^2 = 0.0996$ and $\chi_{Y/X}^2 = 3.867$; 10^{-6} M dTC (■), $\chi_Y^2 = 0.029$ and $\chi_{Y/X}^2 = 2.801$. Binding constants for AcCh in the absence of dTC: $K_R = 1.2 \times 10^{-8}$ M, $c = 0.072$, and $L = 1.8$. In the presence of dTC: $K_{R\alpha} = 1.2 \times 10^{-8}$ M, $K_{R\beta} = 2 \times 10^{-6}$ M, $c = d = 0.072$, and $L = 1.8$. Binding constants for dTC: $K_{R\delta} = 3.5 \times 10^{-8}$ M, $K_{R\varepsilon} = 4 \times 10^{-7}$ M, $e = g = 0.3$.

absence of dTC (Figure 4). It therefore appears that all the dTC inhibition is reversible.

The inhibition pattern obtained with decamethonium was different from either nicotine or dTC; the inhibition pattern appeared to have features of both (Figure 5): the inhibition not only resulted in a curvilinearity in the Scatchard plot similar to the observed with dTC, but also changed the slope of the remaining high affinity binding as observed with nicotine.

Theoretical Section

Because the Hill coefficients of AcCh binding were from 1.3 to 2.0, the blockade of [^{3}H]AcCh binding by nicotine, dTC, and decamethonium should be examined with respect to a cooperative binding model. We chose the two-state or allosteric model of Monod et al. (1965) because it had been applied to electrophysiological data (Karlin, 1967; Edelstein, 1972) with reasonable success. The action of dTC on electrophysiological preparations has also been described by the two-state model (Podleski, 1973).

In the two-state model, the oligomeric protein is proposed to exist in two conformations, the R state in which each protomer (monomer with one site for ligand in a cooperative oligomer) has a high affinity for ligand and the T state in which each protomer exhibits lower affinity for the ligand. The dissociation constants for the R and T states are represented by K_R and K_T, respectively. In the absence of ligand the two states are in equilibrium; the equilibrium constant is $L = (T)/(R)$. The transition from T to the R state is concerted, i.e., there are no hybrid states in which protomers of the same oligomer have both affinities, K_R and K_T. When L is greater than 1 and the ratio of dissociation constants, $c = K_R/K_T$, is less than 1, cooperative binding to a protein may be observed. The model is described by two equations. The binding of ligand is given by the fractional saturation, $\bar{Y}$:

$$\bar{Y}_\alpha = \frac{\alpha(1+\alpha)^{n-1} + Lc\alpha(1+c\alpha)^{n-1}}{(1+\alpha)^n + L(1+c\alpha)^n} \quad (1)$$

where n is the number of protomers and α is defined as x/K_R in which x is the ligand concentration. The subscript on $\bar{Y}$ is included to emphasize only one class of binding sites in contrast to the expansions described in models I through III. In addition, the fraction of oligomers in the R state is represented by eq 2.

$$\bar{R}_\alpha = \frac{1}{1 + \dfrac{L(1+c\alpha)^n}{(1+\alpha)^n}} \quad (2)$$

At saturating ligand concentrations (when $\bar{Y} = 1$) $\bar{R}$ becomes $\bar{R}_{max}$ and:

$$\bar{R}_{\alpha,max} = \frac{1}{1 + Lc^n} \quad (3)$$

Equation 3 shows that the fraction of oligomers in the R state does not approach 1 so long as Lc^n is much greater than 0. This feature has been used to describe the differences in the maximum response of isolated electroplax cells to carbamylcholine and decamethonium (Edelstein, 1972), assuming a direct relation between $\bar{R}$ and response.

The scheme for simple competitive binding of agonists such as nicotine and acetylcholine has been described by Karlin (1967) and applied to the $\bar{R}$ function. From the same binding

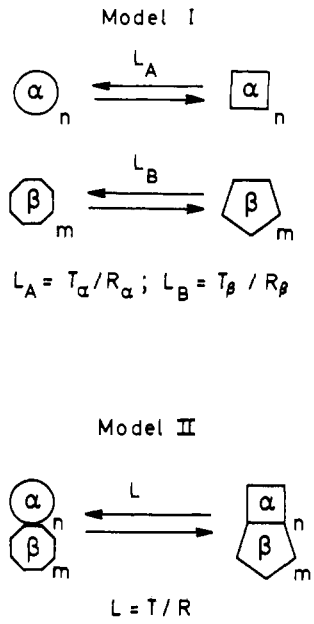

FIGURE 6: Proposed oligomeric structure of AcChR in models I and II.

$$\bar{Y}_{\alpha+\beta} = F_A \frac{\alpha(1+\alpha+\alpha_1)^{l-1} + L_A c\alpha(1+c\alpha+c_1\alpha_1)^{l-1}}{(1+\alpha+\alpha_1)^l + L_A(1+c\alpha+c_1\alpha_1)^l} + F_B \frac{\beta(1+\beta+\beta_1)^{m-1} + L_B d\beta(1+d\beta+d_1\beta_1)^{m-1}}{(1+\beta+\beta_1)^m + L_B(1+d\beta+d_1\beta_1)^m} \quad (6)$$

where F_A and F_B are the fractional amounts of oligomer A and oligomer B ($F_A + F_B = 1$). The fraction of oligomers in the R state is given by eq 7:

$$\bar{R}_{\alpha+\beta} = F_A \frac{1}{1 + \frac{L_A(1+c\alpha+c_1\alpha_1)^l}{(1+\alpha+\alpha_1)^l}} + F_B \frac{1}{1 + \frac{L_B(1+d\beta+d_1\beta_1)^m}{(1+\beta+\beta_1)^m}} \quad (7)$$

Figure 7a, b shows the expected binding of an agonist (AcCh in this case) that binds with equal affinity to oligomers A and B ($K_{R\alpha} = K_{R\beta}$) in the presence of an inhibitor that essentially binds only to oligomer A, i.e., $K_{Ri} \ll K_{Rj}$. By setting $F_A = F_B$ and $l = m$ in eq 6, the competitive inhibitor will block up to 50% of the AcCh binding, thus approximating the effect of dTC inhibition. When the inhibitor binds to oligomer A as an antagonist, i.e., $c_1 > 1$ where $c_1 = K_{Ri}/K_{Ti}$, the binding curves in Figure 7a were obtained that clearly do not resemble dTC inhibition. However, when the inhibitor binds as an agonist, i.e., $c_1 < 1$, the theoretical curves (Figure 7b) are qualitatively similar to dTC inhibition. However, the quantitative fit is relatively poor as can be seen by comparison with the experimental data (included in Figure 7b to facilitate comparison). At 10^{-7} M dTC, $\chi_Y^2 = 0.168$ and $\chi_{Y/X}^2 = 11.07$; at 10^{-6} M dTC, $\chi_Y^2 = 0.184$ and $\chi_{Y/X}^2 = 13.29$.

It is readily apparent that eq 6 and 7 reduce to eq 4 and 5 when $\alpha = \beta$, $\alpha_1 = \beta_1$, $l = m$, and $L_A = L_B$.

Model II. A second possibility is that the receptor population is homogeneous but that each oligomer is made up of both α and β protomers (Figure 6). Each protomer has a single binding site for ligand and inhibitor in the T and R states. We may therefore define all the parameters for ligand and inhibitor binding as in model I. Since there is only one class of oligomer, $\alpha_l\beta_m$, there is only one equilibrium constant for the T and R states, which is defined as in eq 1. The difference between models I and II results in a considerable change in the $\bar{Y}$ and $\bar{R}$ functions. The equations for the fractional saturation, $\bar{Y}_{\alpha\beta}$, and the state function, $\bar{R}_{\alpha\beta}$, are rather long and the derivations are given in the Appendix (eq A11 and A12, respectively).

The expected binding of AcCh in the presence of a competitive inhibitor that blocks binding to only the α protomers ($K_{Ri} \ll K_{Rj}$ in eq A11 of the Appendix) is presented in Figure 7c,d. The number of α and β protomers is assigned as equal ($l = m$) for the reasons presented in model I. When the inhibitor binds as an antagonist, i.e., $c_1 > 1$, the curves in Figure 7c were obtained and do not have the same appearance as the dTC inhibited AcCh binding. Binding of the inhibitor as an agonist ($c_1 < 1$) is presented in Figure 7d and the theoretical curves qualitatively resemble the experimental data. The quantitative fit is better than in model I (Figure 7b): at 10^{-7} M dTC, $\chi_Y^2 = 0.112$ and $\chi_{Y/X}^2 = 9.04$; at 10^{-6} M dTC, $\chi_Y^2 = 0.140$ and $\chi_{Y/X}^2 = 4.21$. The experimental data are included to facilitate comparison.

Model III. This model is different from models I and II in that it proposes a class of inhibitors that bind to allosteric sites, thus altering a fraction of the agonist binding sites to a form with lower affinity for the agonist. Binding of AcCh in the absence of dTC is described by $\bar{Y}_\alpha$ (eq 1); at saturating concentrations of dTC the binding of AcCh exhibits equal amounts of high- and low-affinity binding. This binding is described by $\bar{Y}^*$ (eq A18 in the Appendix) where $K_{R\alpha} \ll K_{R\beta}$. This differs from models I and II where the AcCh dissociation constants are the same even in the presence of the inhibitor. The inhibitor binds to sites that are different from the AcCh-binding sites and its binding is given by $\bar{Y}_{\delta\sigma}$. The $\bar{Y}_{\delta\sigma}$ function for dTC binding is for a positively cooperative system that exhibits half-of-site binding, i.e., $K_{R\delta} \neq K_{R\sigma}$ (see Discussion). Acetylcholine binding in the presence of the allosteric inhibitor is given by eq 8:

$$\bar{Y}_{all.} = \bar{Y}_\alpha(1 - \bar{Y}_{\delta\sigma}) + \bar{Y}_{\delta\sigma}(\bar{Y}^*) \quad (8)$$

If the inhibitor also binds competitively, as suggested in decamethonium blockade, $\bar{Y}_c$ is substituted for $\bar{Y}_\alpha$. The state function is similarly given by eq 9:

$$\bar{R}_{all.} = \bar{R}_\alpha(1 - \bar{R}_{\delta\sigma}/\bar{R}_{\delta\sigma(max)}) + (\bar{R}_{\delta\sigma}/\bar{R}_{\delta\sigma(max)})(\bar{R}^*) \quad (9)$$

where $\bar{R}_\alpha$ and $\bar{R}^*$ are given by eq 2 and A19 (in Appendix), respectively. The state function of the inhibitor is given by $\bar{R}_{\delta\sigma}$ and at $\bar{Y}_{\delta\sigma} = 1$ becomes $\bar{R}_{\delta\sigma(max)}$. The R* state may represent a conducting state; however, due to the altered binding affinities for agonist ($K_{R\alpha} \neq K_{R\beta}$), the $\bar{R}^*$ function approaches $\bar{R}^*_{max}$ at a much higher concentration of agonist than required for $\bar{R}_\alpha$. Since $\bar{R}^*_{max} = 1/(1 + Lc^l d^m)$, when $c = d$ and $l = m$, $\bar{R}^*_{max}$ equals $\bar{R}_{\alpha,max}$. Thus, the allosteric inhibitor will produce an apparent competitive blockade of the response.

The theoretical curves in Figures 3 and 4 for dTC inhibition were generated by eq 8. The AcCh binding constants used were $K_{R\alpha} = 1.2 \times 10^{-8}$ M and $K_{R\beta} = 2 \times 10^{-6}$ M; c and d are 0.072. The dissociation constants assumed for dTC were $K_{R\delta} = 3.5 \times 10^{-8}$ M and $K_{R\sigma} = 4.0 \times 10^{-7}$ M; e and g are 0.3 (definitions of the dTC inhibition parameters are given in the footnotes of Table I); at 10^{-7} M dTC, $\chi_Y^2 = 0.101$ and $\chi_{Y/X}^2 = 3.87$; at 10^{-6} M dTC, $\chi_Y^2 = 0.030$ and $\chi_{Y/X}^2 = 2.80$.

Discussion

Evaluation of Models. The two-state model for cooperative ligand binding has produced excellent descriptions of [^{3}H]AcCh binding to the solubilized AcChR presented in

TABLE I: Dissociation Constants (μM) for Cholinergic Ligands to Triton-Solubilized AcChR.

	Agonist Site				Allosteric Site			
	$K_{R\alpha}$[a]	$K_{R\beta}$[b]	c[c]	d[d]	$K_{R\delta}$[e]	$K_{R\sigma}$[f]	e[g]	g[h]
AcCh	0.012	0.012	0.072	0.072				
AcCh[i]	0.012	2.0	0.072	0.072				
Nicotine	0.5	0.5	0.1	0.1				
dTC					0.035	0.40	0.3	0.3
Decamethonium	0.6		0.1		0.35	1.0	0.1	0.1

[a] Dissociation constant for α protomer in R state. [b] Dissociation constant for β protomer in R state. [c] $c = K_{R\alpha}/K_{T\alpha}$; $K_{T\alpha}$ is dissociation constant for α protomer in T state. [d] $d = K_{i\beta}/K_{T\beta}$; $K_{T\beta}$ is dissociation constant for β protomer in T state. [e] Dissociation constant for allosteric site on α protomer in R state. [f] Dissociation constant for allosteric site on β protomer in R state. [g] $e = K_{R\delta}/K_{T\delta}$; $K_{T\delta}$ is dissociation constant for allosteric site on α protomer in T state. [h] $g = K_{R\sigma}/K_{T\sigma}$; $K_{T\sigma}$ is dissociation constant for allosteric site on β protomer in T state. [i] Dissociation constant for AcCh in presence of allosteric inhibition such as in dTC or decamethonium.

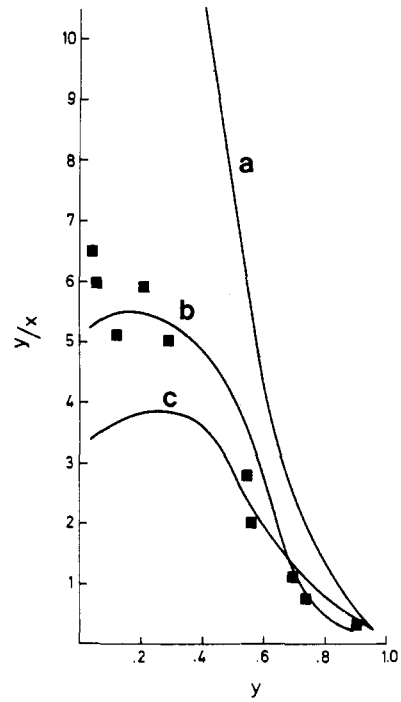

FIGURE 8: Theoretical binding curves generated by model I (c), model II (a), and model III (b). Experimental data for 10^{-6} M dTC inhibition included from Figure 4. Deviation in observed binding and theoretical binding curves are: model I, $\chi_Y^2 = 0.155$ and $\chi_{Y/X}^2 = 7.294$; model II, $\chi_Y^2 = 0.450$ and $\chi_{Y/X}^2 = 14.738$; and model III, $\chi_Y^2 = 0.022$ and $\chi_{Y/X}^2 \doteq 0.539$.

fit using eq 8 of model III. It should be noted that the equilibrium constant, L, was the only parameter varied to obtain the theoretical inhibition curves for the data in Figure 3 (L = 1.9) and Figure 4 (L = 1000). By contrast, when L was increased from 1.9 to 1000 in models I and II, holding all other parameters constant, the theoretical inhibition curves deviated considerably from the experimental data (Figure 8). Thus, while competitive inhibition of AcCh binding to only one class of nonidentical protomers may produce Scatchard plots with apparent "negative" cooperativity, the third model produced the best quantitative description of dTC inhibition.

Decamethonium inhibition of [^{3}H]AcCh binding was fitted by eq 8 of model III where $\bar{Y}_c$ (eq 4) was substituted for $\bar{Y}_\alpha$ (eq 1) to account for the competitive component. The quality of the theoretical fits are given by the χ^2 values in the legend of Figure 5. The binding constants thus obtained for nicotine, dTC, and decamethonium are summarized in Table I.

Implications of Inhibition Studies. The results of the drug inhibition studies are quite dramatic: nicotine, an agonist, bound as a competitive inhibitor; dTC apparently induced or stabilized a conformation of the AcChR that exhibited "half-of-site" binding of AcCh; decamethonium showed less specificity and bound to both the AcCh site and the dTC allosteric site.

The blockade by dTC of the depolarization caused by agonists has been interpreted in the two-state model as preferential binding of dTC to the T state (Podleski, 1973). Such binding would not exhibit positive cooperativity. However, the cooperative binding of dTC has been implied in the cases of its interaction with isolated electroplax cells (Changeux and Podleski, 1968) and excitable microsacs (Kasai and Changeux, 1971). Also, Eldefrawi and Eldefrawi (1971) observed positive cooperativity in the binding of [^{14}C]dTC to particulate preparations from *Electrophorus electricus* and to highly purified preparations of AcChR from *T. marmorata* (personal communication). Preliminary studies (Gibson, unpublished) on crude receptor preparations of *T. californica* indicated positive cooperativity in the binding of [^{14}C]dTC with $K_R = 4 \times 10^{-8}$ M and maximal binding of less than or equal to half of that observed for [^{3}H]AcCh to the same preparation. The cooperative binding of dTC in model III will produce an apparent competitive blockade of the agonist-induced depolarization by reducing the fraction of oligomers in the R state according to eq 9. By contrast, the cooperative binding of dTC in models I and II ($c_1 < 1$) would result in a facilitation of the agonist-induced response, a condition which is clearly not seen electrophysiologically. Additional evidence favoring model III for dTC binding is that it implies allosteric binding that exhibits half-of-site affinity ($K_{R\delta}$ and $K_{R\sigma}$ in Table I). Allosteric binding of dTC has in fact been postulated on the basis of physiological studies (Silman and Karlin, 1969) and half-of-site binding of dTC has been proposed on the basis of in vitro binding studies (Fu et al., 1974).

With respect to decamethonium inhibition, the competitive and allosteric behavior that are evident tempt one to suggest that the depolarization caused by decamethonium is the result of the competitive component, and the subsequent blockade is a result of the allosteric component. This dual action has been inferred with respect to decamethonium in studies on excitable microsacs (Kasai and Changeux, 1971). However, the blockade produced by dTC and decamethonium are quite different, the latter apparently resulting from agonist-induced desensitization of the muscle end plates (Thesleff, 1955a,b).

Comparisons with Electrophysiological Studies. The apparent positive cooperativity of the electrophysiological re-

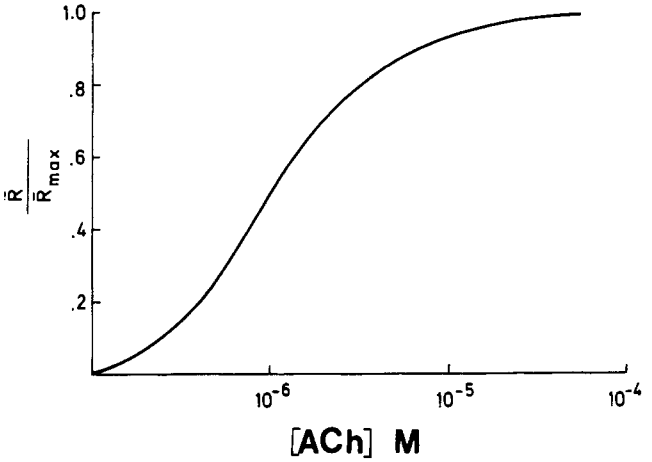

FIGURE 10: Theoretical dose-response curve for AcCh. $K_R = 2 \times 10^{-8}$ M, $c = 0.07$, and $L = 80\,000$. Note that the half-maximal response occurs at 1×10^{-6} M.

AcCh. In addition, the lowered affinity to half-of-the-sites for AcCh would increase the off-rate. As such termination of the depolarization would be influenced by the increase in concentration of a regulatory substance during the rising phase of depolarization. Good candidates for the regulatory substance are Ca^{2+}, K^+ or a change in the local pH.

Additionally, model III allows for a third state that exhibits properties unlike either the T or R states, i.e., half-of-site binding of AcCh. Such a state may be related to the third state postulated by Katz and Thesleff (1957) to rationalize desensitization of the electrophysiological response to agonists.

Acknowledgments

The author thanks Dr. R. D. O'Brien, in whose laboratory this work was completed, S. J. Edelstein for assistance in the preparation of this manuscript, and their many helpful discussions. The author also thanks Dr. T. R. Podleski and B. Land for their many conversations that helped lead to the completion of this work.

Appendix

The binding of ligand to nonequivalent sites has recently been treated by Edelstein (1974) in an extension of the allosteric model of Monod et al. (1963). Although the equations described only the $\alpha_2\beta_2$ system of hemoglobin (Hgb), the equations can be easily generalized to describe ligand binding to $\alpha_l\beta_m$ (Scheme IA) in which α sites bind ligand, x, with a dissociation constant of $K_{R\alpha}$ in the R state and $K_{T\alpha}$ in the T state; the β sites exhibit dissociation constants for ligand of $K_{R\beta}$ and $K_{T\beta}$ for the R and T states, respectively. The equilibria in Scheme IA can be expressed as:

$$T_{\beta_0}{}^{\alpha_0} = LR_{\beta_0}{}^{\alpha_0} \tag{A1}$$

where L is the equilibrium constant between the two states and the subscripts on the α and β indicate the number of ligand molecules bound, and:

$$R_{\beta_j}{}^{\alpha_i} = R_{\beta_0}{}^{\alpha_0} \frac{l!}{(l-i)!\,i!} \frac{m!}{(m-j)!\,j!} \left[\frac{x}{K_{R\alpha}}\right]^i \left[\frac{x}{K_{R\beta}}\right]^j \tag{A2}$$

The fractional saturation, $\bar{Y}$, and the fraction of oligomers in the R state, $\bar{R}$, are defined by eq A3 and A4:

SCHEME IA

$$T_{\beta_0}{}^{\alpha_0} \overset{L}{\rightleftharpoons} R_{\beta_0}{}^{\alpha_0}$$

$$\begin{aligned}
T_{\beta_0}{}^{\alpha_0} + x &\overset{K_{T\alpha}}{\rightleftharpoons} T_{\beta_0}{}^{\alpha_1} & R_{\beta_0}{}^{\alpha_0} + x &\overset{K_{R\alpha}}{\rightleftharpoons} R_{\beta_0}{}^{\alpha_1}\\
T_{\beta_0}{}^{\alpha_0} + x &\overset{K_{T\beta}}{\rightleftharpoons} T_{\beta_1}{}^{\alpha_0} & R_{\beta_0}{}^{\alpha_0} + x &\overset{K_{R\beta}}{\rightleftharpoons} R_{\beta_1}{}^{\alpha_0}\\
T_{\beta_0}{}^{\alpha_1} + x &\overset{K_{T\beta}}{\rightleftharpoons} T_{\beta_1}{}^{\alpha_2} & R_{\beta_0}{}^{\alpha_1} + x &\overset{K_{R\beta}}{\rightleftharpoons} R_{\beta_1}{}^{\alpha_2}\\
T_{\beta_1}{}^{\alpha_0} + x &\overset{K_{T\alpha}}{\rightleftharpoons} T_{\beta_1}{}^{\alpha_1} & R_{\beta_1}{}^{\alpha_0} + x &\overset{K_{R\alpha}}{\rightleftharpoons} R_{\beta_1}{}^{\alpha_1}\\
&\vdots & &\vdots\\
T_{\beta_{j-1}}{}^{\alpha_{i-1}} + x &\overset{K_{T\alpha}}{\rightleftharpoons} T_{\beta_{j-1}}{}^{\alpha_i} & R_{\beta_{j-1}}{}^{\alpha_{i-1}} + x &\overset{K_{R\alpha}}{\rightleftharpoons} R_{\beta_{j-1}}{}^{\alpha_i}\\
T_{\beta_{j-1}}{}^{\alpha_{i-1}} + x &\overset{K_{T\beta}}{\rightleftharpoons} T_{\beta_j}{}^{\alpha_{i-1}} & R_{\beta_{j-1}}{}^{\alpha_{i-1}} + x &\overset{K_{R\beta}}{\rightleftharpoons} R_{\beta_j}{}^{\alpha_{i-1}}\\
T_{\beta_j}{}^{\alpha_{i-1}} + x &\overset{K_{T\alpha}}{\rightleftharpoons} T_{\beta_j}{}^{\alpha_i} & R_{\beta_j}{}^{\alpha_{i-1}} + x &\overset{K_{R\alpha}}{\rightleftharpoons} R_{\beta_j}{}^{\alpha_i}\\
T_{\beta_{j-1}}{}^{\alpha_i} + x &\overset{K_{T\beta}}{\rightleftharpoons} T_{\beta_j}{}^{\alpha_i} & R_{\beta_{j-1}}{}^{\alpha_i} + x &\overset{K_{R\beta}}{\rightleftharpoons} R_{\beta_j}{}^{\alpha_i}
\end{aligned}$$

$$\bar{Y} = \frac{\sum_{\substack{i=0\\(i+j\neq 0)}}^{l}\sum_{j=0}^{m}(i+j)\,R_{\beta_j}{}^{\alpha_i} + \sum_{\substack{i=0\\(i+j\neq 0)}}^{l}\sum_{j=0}^{m}(i+j)\,T_{\beta_j}{}^{\alpha_i}}{(l+m)\left(\sum_{i=0}^{l}\sum_{j=0}^{m}R_{\beta_j}{}^{\alpha_i} + \sum_{i=0}^{l}\sum_{j=0}^{m}T_{\beta_j}{}^{\alpha_i}\right)} \tag{A3}$$

$$\bar{R} = \frac{\sum_{i=0}^{l}\sum_{j=0}^{m}R_{\beta_j}{}^{\alpha_i}}{\sum_{i=0}^{l}\sum_{j=0}^{m}R_{\beta_j}{}^{\alpha_i} + \sum_{i=0}^{l}\sum_{j=0}^{m}T_{\beta_j}{}^{\alpha_i}} \tag{A4}$$

By substituting eq A1 and A2 into A3 and A4, defining $\alpha = x/K_{R\alpha}$, and $\beta = x/K_{R\beta}$, $c = K_{R\alpha}/K_{T\alpha}$ and $d = K_{R\beta}/K_{T\beta}$, eq A5 and A6 are obtained:

$$\bar{Y} = \frac{\begin{aligned}&l\alpha(1+\alpha)^{l-1}(1+\beta)^m + m\beta(1+\beta)^{m-1}(1+\alpha)^l\\ &+ L[lc\alpha(1+c\alpha)^{l-1}(1+d\beta)^m\\ &+ md\beta(1+d\beta)^{m-1}(1+c\alpha)^l]\end{aligned}}{(l+m)[(1+\alpha)^l(1+\beta)^m + L(1+c\alpha)^l(1+d\beta)^m]} \tag{A5}$$

$$\bar{R} = \frac{1}{1 + \dfrac{L(1+c\alpha)^l(1+d\beta)^m}{(1+\alpha)^l(1+\beta)^m}} \tag{A6}$$

When $l = m = 2$, eq A5 and A6 reduce to the equations derived by Edelstein to describe ligand binding to Hgb (1974). In addition, when $\alpha = \beta$ and $l = m$, eq A5 and A6 reduce to eq 1 and 2 in the text.

Equations A5 and A6 do not, however, describe competitive or allosteric inhibition of ligand binding to nonidentical protomers. Descriptions of competitive binding by a second ligand (Karlin, 1967) and allosteric binding (Rubin and Changeux, 1966) have been presented with respect to the $\bar{R}$ function. Since their discussions did not include the $\bar{Y}$ function or ligand binding to nonequivalent protomers, a rigorous description of each system follows.

Competitive binding of a second ligand, I, to nonequivalent protomers is presented in Scheme IIA, where $i + h \leq l$ and $j + k \leq m$. By defining the dissociation constants for the second ligand as K_{Ri} and K_{Rj} for the α and β sites, respectively, we can represent the equilibria in Scheme IIA by eq A1, A7, and A8: